

Received September 8, 2019, accepted October 13, 2019, date of publication October 16, 2019, date of current version October 29, 2019.

Digital Object Identifier 10.1109/ACCESS.2019.2947623

# A Hybrid Internet/CATV/5G Fiber-FSO Integrated System With a Triple-Wavelength Polarization Multiplexing Scenario

CHUNG-YI LI<sup>1</sup>, HSIAO-WEN WU<sup>2</sup>, HAI-HAN LU<sup>3</sup>, (Senior Member, IEEE), WEN-SHING TSAI<sup>4</sup>, SONG-EN TSAI<sup>3</sup>, AND JING-YAN XIE<sup>3</sup>

<sup>1</sup>Department of Communication Engineering, National Taipei University, New Taipei City 237, Taiwan

<sup>2</sup>Department of Electronic Engineering, Tunghan University, New Taipei City 222, Taiwan

<sup>3</sup>Institute of Electro-Optical Engineering, National Taipei University of Technology, Taipei 106, Taiwan

<sup>4</sup>Department of Electrical Engineering, Ming Chi University of Technology, New Taipei City 243, Taiwan

Corresponding author: Hai-Han Lu (hhlu@ntut.edu.tw)

This work was supported by the Qualcomm-NTUT Research Project under Grant NAT-414684.

**ABSTRACT** A hybrid Internet/cable television (CATV)/5G fiber-free-space optical (FSO) integrated system with a triple-wavelength polarization multiplexing scenario is attainably demonstrated for the first time. In a triple-wavelength polarization multiplexing scenario with vestigial sideband (VSB) four-level pulse amplitude modulation (PAM4)/CATV/16-quadrature amplitude modulation (QAM)-orthogonal frequency-division multiplexing (OFDM) modulation, the channel capacity is considerably multiplied and the overall performance is significantly improved. With a tunable optical band-pass filter, polarization-tracking free de-multiplexing is attained by removing other wavelengths with different polarizations, and the optical VSB PAM4/CATV/16-QAM-OFDM signal is created by partially reducing the optical signal's linewidth. Compared with established polarization multiplexing fiber-FSO integrations with complex polarization de-multiplexing mechanism, it demonstrates a notable one with the benefits of simplicity and flexibility. Sufficiently low bit error rate, acceptable PAM4 eye diagrams, clear constellation map, and high composite second-order/composite triple beat values are attained through a 40 km single-mode fiber transport with 200 m free-space link. This demonstrated triple-wavelength polarization multiplexing fiber-FSO integrated system is promising because it not only incorporates fiber backhaul with optical wireless feeder, but it also simplifies system's structure and enhance system's overall performance.


**INDEX TERMS** Fiber-FSO integrated system, optical VSB filter, polarization multiplexing scenario, tunable optical band-pass filter, triple-wavelength.

## I. INTRODUCTION

Along with the increasing popularity of Internet, cable television (CATV), and mobile telecommunication applications, data center interconnection traffic is growing exponentially. This exponential growth of interconnection loading has driven the need for high transmission capacity. Polarization multiplexing scenario closely matches the optical backhaul of fiber free-space optical (FSO) integrated systems and has been investigated for providing broadband integrated services [1]–[3]. Fiber-FSO integrated systems have attracted substantial attention for linking fiber-backhaul and optical wireless feeders [4]–[7]. They can cover service areas at

comparatively fast speed and low cost by utilizing the features of optical fiber and optical wireless communications, such as the inherently huge bandwidth of optical fiber and the unlicensed electrical spectrum of optical wireless communication. Accordingly, fiber-FSO integrated systems present a strong platform for the supporting and generating present and developing applications, such as high-speed Internet, cloud services, 4k/8k HDTV, CATV broadband communication, and 5G mobile telecommunication [8]–[12]. In comparison with other communication systems, fiber-FSO integrated systems with a polarization multiplexing scenario not only provide broadband convergent services, but also offer sufficient mobility.

In this study, a hybrid Internet/CATV/5G fiber-FSO integrated system through 40 km single-mode fiber (SMF)

The associate editor coordinating the review of this manuscript and approving it for publication was Lei Guo .

transport with 200 m free-space transmission is proposed, using a triple-wavelength polarization multiplexing scenario as a demonstration. The lights are modulated with 60 Gb/s vestigial sideband (VSB) four-level pulse amplitude modulation (PAM4) (Internet), 50–550 MHz VSB-CATV even-channel, and 70 Gb/s VSB 16-quadrature amplitude modulation (QAM)-orthogonal frequency-division multiplexing (OFDM) (5G) signals to satisfy the target of broadband heterogeneous services. The PAM4 and 16-QAM-OFDM signals may not be simply regarded as Internet and 5G data, respectively. In order to maximize the data rate and match the signal formats, however, PAM4 (baseband) and 16-QAM-OFDM (passband) signals are regarded as Internet (baseband) and 5G (passband) data in this hybrid integrated system. The spectrum of PAM4 is half as wide as that of the non-return-to-zero signal, making PAM4 modulation promising in high capacity links [13], [14]. CATV modulation has been developed extensively for broadband transmissions. As for 16-QAM-OFDM modulation, it is an effectual scheme with high spectrum efficiency, high transmission capacity, and powerful dispersion tolerance [15]. For a 40-km SMF transport with 200-m free-space transmission and given quality requirements, the realization of such a hybrid Internet/CATV/5G fiber-FSO integrated system with different signal formats is challenging. Since PAM4/CATV/16-QAM-OFDM signal has large linewidth and brings significant fiber dispersion in fiber-FSO integrated systems, yet VSB PAM4/CATV/16-QAM-OFDM signal is used to improve the dispersion tolerance because the optical signal spectrum has been reduced [16]–[19]. In addition, the adoption of a polarization multiplexing scenario is effective for carrying different signals and enhancing the transmission capacity [20]–[23]. Three wavelengths are polarized in different polarizations ( $x$ -polarization, polarization rotated at a  $45^\circ$  angle to the  $x$ -axis, and  $y$ -polarization). The channel capacity of a hybrid Internet/CATV/5G fiber-FSO integrated system can be substantially multiplied by combining VSB PAM4/CATV/16-QAM-OFDM modulation and a triple-wavelength polarization multiplexing scenario. Hybrid Internet/CATV/5G fiber-FSO integrated systems would be attractive for broadband networks to provide full services including high-speed Internet, broadband CATV, and 5G mobile telecommunication.

For conventional lightwave transport systems with a polarization multiplexing scenario, a costly and complicated polarization de-multiplexing mechanism is needed to separate each polarization [24]–[27]. Xiang *et al.* demonstrated a modulation-transparent and joint polarization and phase-tracking scheme [24]. However, sophisticated nonlinear principal component analysis is needed to acquire joint polarization and phase-tracking. Li *et al.* achieved a polarization-tracking scheme based on polarization phase locking least mean square algorithm [25]. Matsuda *et al.* developed polarization multiplexing and de-multiplexing techniques to increase the transmission capacity of optical module [26]. Nevertheless, complex digital signal processing

schemes are required to obtain each polarization. Su *et al.* obtained a bidirectional multiband radio-over-fiber (RoF) system based on polarization multiplexing and wavelength reuse [27]. Multiple polarization controllers and polarizers involved at the receiver side to de-multiplex the polarized optical carriers make RoF systems more complicated. Developing a polarization de-multiplexing approach with low cost and low complexity is thereby imperative for a polarization multiplexing lightwave transport system. Tunable optical band-pass filter (TOBPF) is a simple and feasible polarization de-multiplexing mechanism. It is attractive because it avoids the need of expensive and complex polarization de-multiplexing mechanism. With the adoption of polarization-independent TOBPF with variable bandwidth, the polarized wavelengths are easily de-multiplexed in each polarization state because they are modulated at different wavelengths. Polarization-tracking free de-multiplexing is achieved by removing other wavelengths with different polarizations. Moreover, the TOBPF also operates as an optical VSB filter. The optical PAM4/CATV/16-QAM-OFDM signal's linewidth will be partially reduced by an optical VSB filter to produce optical VSB PAM4/CATV/16-QAM-OFDM signal. TOBPF not only functions as a simple polarization de-multiplexing mechanism to de-multiplex the polarized wavelengths but also operates as an optical VSB filter to ameliorate the fiber dispersion.

We attainably constructed a hybrid Internet/CATV/5G fiber-FSO integrated system with a triple-wavelength polarization multiplexing scenario. The feasibility of delivering polarization-division-multiplexing (PDM) PAM4/16-QAM-OFDM hybrid signals with OBPFs to de-multiplex the two orthogonal polarization states has been demonstrated [28], [29]. Through PDM scenario and parallel/orthogonally polarized single-wavelength operation, the transmission capacity is doubled. However, some undesired signals exist in each receiving due to parallel/orthogonally polarized single-wavelength operation. Instead of employing single-wavelength operation, triple-wavelength operation is a prominent way to reduce the undesired signals induced by parallel/orthogonally polarized wavelengths. Sufficiently low bit error rate (BER), acceptable PAM4 eye diagrams, clear constellation map, and good composite second-order (CSO)/composite triple beat (CTB) performance are obtained through 40 km SMF transport and 200 m free-space transmission. It shows a noteworthy system with the benefits of simplicity and flexibility, as compared to polarization multiplexing fiber-FSO integrated systems with complicated polarization de-multiplexing mechanism.

## II. EXPERIMENT

### A. STRUCTURE OF THE PROPOSED HYBRID INTERNET/CATV/5G FIBER-FSO INTEGRATED SYSTEM WITH TRIPLE-WAVELENGTH POLARIZATION MULTIPLEXING SCENARIO

The structure of the proposed hybrid Internet/CATV/5G fiber-FSO integrated system with a triple-wavelength

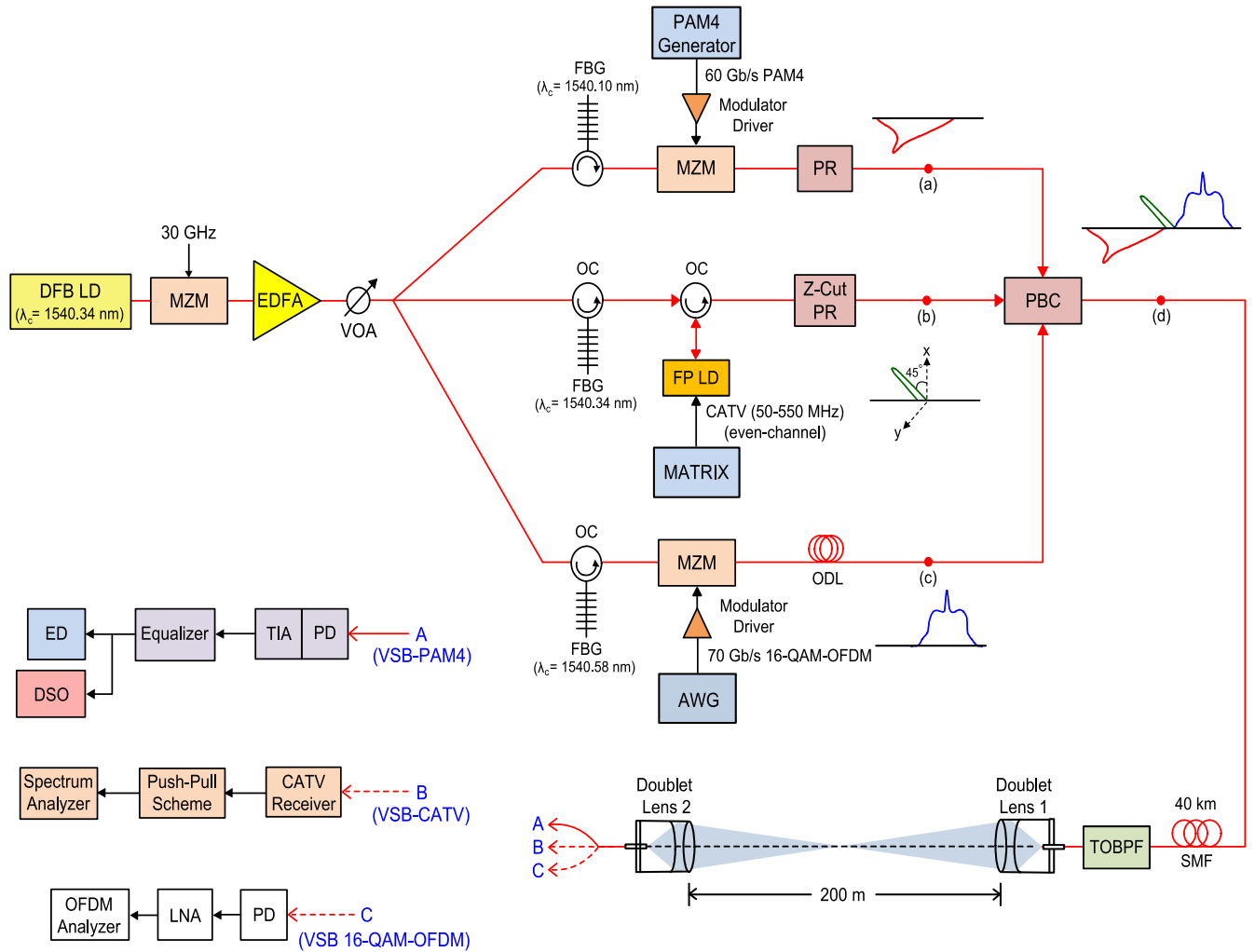


**FIGURE 1.** The structure of the proposed hybrid Internet/CATV/5G fiber-FSO integrated system with a triple-wavelength polarization multiplexing scenario.

polarization multiplexing scenario through 40 km SMF transport and 200 m free-space link is exhibited in Fig. 1. The output of the distributed feedback (DFB) laser diode (LD), with a central wavelength of 1540.34 nm, is sent to a Mach-Zehnder modulator (MZM). The MZM is driven by a 30-GHz RF signal. The optical signal is modulated with the format of a central carrier (zero-order) with double sidebands (first-order sidebands). When the optical signal is modulated by a MZM driven by a RF signal, several sidebands will be created. A proper RF signal is utilized to drive the MZM, bringing about small second-order sidebands after modulation. Only the first-order sidebands are created, and the peak of the first-order sideband is 30 GHz away from the central carrier. If a smaller channel spacing of 15 GHz exists (MZM is driven by a 15-GHz RF signal), it will be a great challenge in such closely spaced optical wavelengths to filter each wavelength. If a larger channel spacing of 40 GHz exists (MZM is driven by a 40-GHz RF signal), it will increase system's cost due to the need of 40 GHz RF signal generator and reduce

the spectral efficiency because of the requirement of wider spectral width. To have an optimum balance among wavelength filtered ability, system's cost, and spectral efficiency, the channel spacing in this proposed hybrid integrated system is set at 30 GHz. The optical signal is then promoted using an erbium-doped fiber amplifier (EDFA), attenuated using a variable optical attenuator (VOA), and separated using a 1×3 optical splitter. As the input power is 0 dBm, the EDFA output power and noise figure are 17 dBm and 4.5 dB, respectively. VOA is located at the start of the fiber-FSO integrated system to attenuate the optical power and bring on fewer distortions because less optical power will be launched into the fiber. For the upper route, the lower sideband (-1 sideband) is reflected by a combination of an optical circulator (OC) and fiber Bragg grating (FBG,  $\lambda_c = 1540.10$  nm), and sent to a 40-GHz MZM. The FBG is characterized by a bandwidth of 0.1 nm and a reflectivity of 0.97. After passing through a modulator driver, a 60 Gb/s PAM4 (Internet) signal generated from a PAM4 generator (Anrisu MP1800A) is

employed to modulate the MZM. MZM's output is then sent to a polarization rotator (PR) to rotate the polarization from  $x$ -polarization to  $y$ -polarization [inset (a)]. For the middle route, the central carrier is chosen via an integration of OC and FBG ( $\lambda_c = 1540.34$  nm) and injected into a Fabry-Perot (FP) LD through an OC. The injection locking technique improves the intensity of the injection-locked sideband and suppresses other sidebands simultaneously. Channels 2 to 78 (CATV even-channel) generated from a multiple signal generator (MATRIX SX-16) are directly supplied to the FP LD. The output of injection-locked FP LD is then inputted into a Z-cut PR to rotate the polarization from  $x$ -polarization to polarization rotated at a  $45^\circ$  angle to the  $x$ -axis [inset (b)]. Notably, a temperature controller is employed to avoid wavelength shift in the FP LD due to temperature variation. As for the lower route, the upper sideband (+1 sideband) is selected by a combination of the OC and FBG ( $\lambda_c = 1540.58$  nm), and inputted into a 40-GHz MZM. After travelling through a modulator driver, a 70 Gb/s 16-QAM-OFDM (5G) signal generated from an arbitrary waveform generator (Tektronix AWG 70001A) is adopted to modulate the MZM. MZM's output is launched into an optical delay line to make up for the phase difference [inset (c)]. Afterward, these 60 Gb/s PAM4 ( $y$ -polarization), 50–550 MHz CATV even-channel (polarization rotated at a  $45^\circ$  angle to the  $x$ -axis), and 70 Gb/s 16-QAM-OFDM ( $x$ -polarization) signals are combined by utilizing a polarization beam combiner. These hybrid signals [inset (d)] are then delivered through the 40 km SMF transport.

Then, these hybrid signals with different polarizations go through a TOBPF to de-multiplex each polarized signal and also reduce the linewidth of each filtered signal. For PAM4 signal ( $y$ -polarization) de-multiplexing, the optical PAM4 signal is de-multiplexed by the TOBPF to generate an optical VSB-PAM4 signal. The TOBPF is characterized by a 0.1-nm bandwidth and a 1200-dB/nm filter slope. For CATV signal (polarization rotated at a  $45^\circ$  angle to the  $x$ -axis) de-multiplexing, the optical CATV signal is de-multiplexed by the TOBPF to produce an optical VSB-CATV signal. In here, the TOBPF is featured by a 0.03-nm narrow bandwidth and a 1500-dB/nm sharp filter slope. As for 16-QAM-OFDM signal ( $x$ -polarization) de-multiplexing, the optical 16-QAM-OFDM signal is de-multiplexed by the TOBPF to generate an optical VSB 16-QAM-OFDM signal. The TOBPF is characterized by a 0.13-nm bandwidth and a 1000-dB/nm filter slope. Thereafter, the de-multiplexed/filtered optical signal is communicated over a 200 m free-space transmission utilizing a couple of doublet lenses, which are deployed to emit laser beam to the free space and to converge laser beam to the fiber's ferrule.

Through 200 m free-space transmission, the filtered 60 Gb/s VSB-PAM4 signal ( $y$ -polarized wavelength) is gotten and promoted by a high-bandwidth photodiode (PD) with a trans-impedance amplifier receiver. After electrical equalization, BER is measured in real-time using a high-sensitivity error detector. Furthermore, a digital storage

oscilloscope is employed to take the eye diagrams of the delivered 60 Gb/s VSB PAM4 signal. For CATV signal, the filtered 50–550 MHz VSB-CATV even-channel signal (polarized wavelength rotated at a  $45^\circ$  angle to the  $x$ -axis) is received by a CATV receiver, sent to a push-pull scheme to suppress nonlinear distortions [30], and supplied in a spectrum analyzer to measure the CSO and CTB values. As for 16-QAM-OFDM signal, the filtered 70 Gb/s VSB 16-QAM-OFDM signal ( $x$ -polarized wavelength) is gotten by a PD, promoted by a low noise amplifier, analyzed by an OFDM analyzer, and post-processed using MATLAB program to evaluate the BER value and the corresponding constellation map.

## B. A COUPLE OF DOUBLET LENSES DEPLOYED FOR 200 M FREE-SPACE TRANSMISSION

A couple of doublet lenses, as shown in the schematic in Fig. 2, are utilized to emit a laser beam to the free-space and to concentrate that laser beam at the fiber's ferrule. The laser beam's transmission through the free space is increased to 200 m ( $50 \text{ m} \times 2 + 25 \text{ m} \times 2$ ) with the support of plane mirrors on four sides. Given that the plane mirrors have high reflectivities above 99.5%, multi-mirror (four-mirror) configuration will not affect the quality of FSO communications. At the receiving end, a convergent scheme must be employed to concentrate the laser beam at the fiber's ferrule. Doublet lens 2 functions as a convergent scheme to couple the laser beam with the fiber's ferrule. Doublet lens, with a 50-mm focal length and a 30-mm diameter, comprises concave and convex lenses paired together. The relation between the spatial frequency cutoff ( $SFC$ ) and the corresponding beam radius ( $r$ ) is stated as:

$$r = 2.3 \times \frac{1}{SFC \times 2\pi} = 3.6(\mu\text{m}) \quad (1)$$

The divergent angle ( $\theta$ ) of laser beam can be counted as:

$$\theta = \frac{3.6(\mu\text{m})}{50(\text{mm})} = 72 \times 10^{-6} \quad (2)$$

Over an  $L$ -m free-space transmission, the diameter of doublet lens 2 must be larger than that of laser beam ( $d_L$ ) ( $30 \text{ mm} > d_L$ ) to comply with the field of view of receiver optics:

$$d_L = \sqrt{d^2 + (2\theta L)^2} = \sqrt{2.2^2 + (0.144L)^2} < 30 \quad (3)$$

$L$  is calculated as 207.8, denoting the maximum possible free-space link. The free-space transmission transported in this demonstration is 200 m to meet the target of maximum free-space transmission. It is critically important to correspond with the beam size to the receiving area through a certain free-space link for decreasing coupling loss and maintaining the free-space transmission workable. A couple of fiber collimators with convex lenses might be employed to substitute a couple of doublet lenses. Nevertheless, it is hard to construct a 200-m free-space transmission using a couple of fiber collimators with convex lenses. The collimated laser

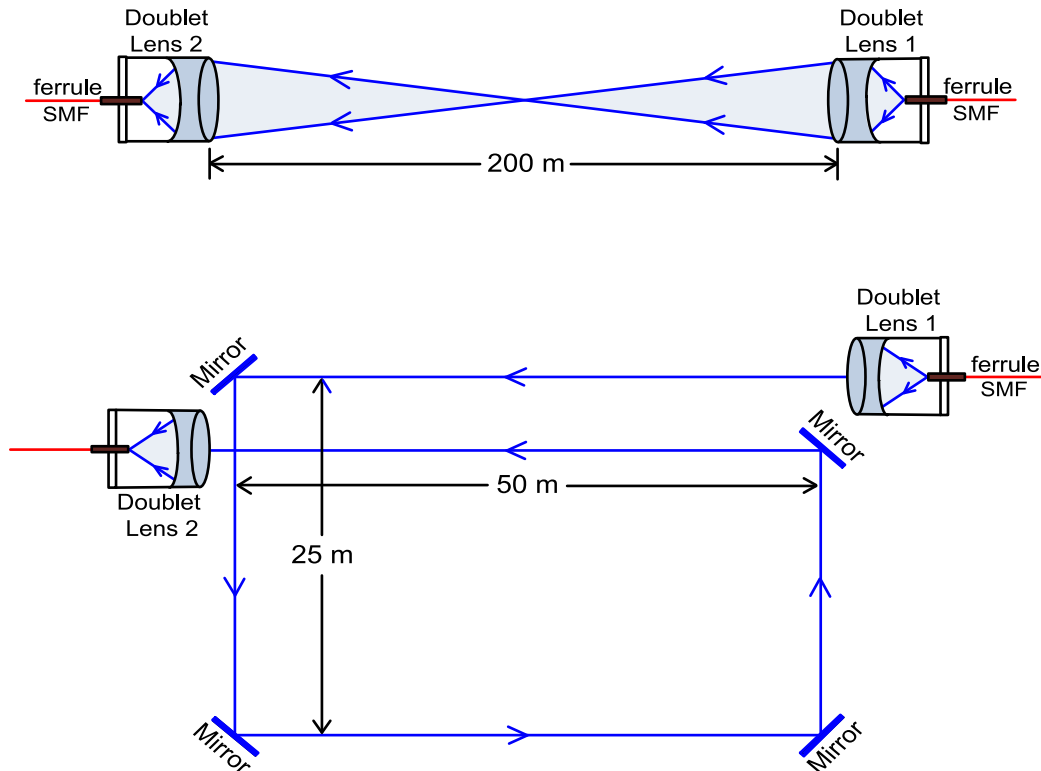


**FIGURE 2.** A couple of doublet lenses is utilized to emit laser beam to the free space and to concentrate the laser beam at the fiber's ferrule.

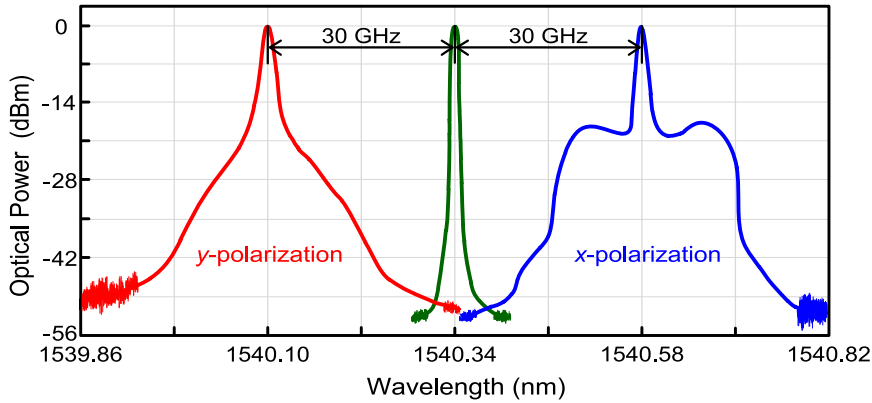
beam sent out from a fiber collimator with a convex lens will expand as it communicates over a certain free-space link. In a free-space transmission of 200 m, the diameter of doublet lens 2 will be smaller than that of laser beam. With large laser beam diameter, the convex lens with fiber collimator at the receiving end will collect less transmitted laser beam. An apparent reduction in the received optical power will occur, accompanied by bad BER performance.

FSO communications are affected by the atmospheric turbulence. The atmospheric turbulence will cause atmospheric attenuation as the optical signal propagates through the free-space link. For FSO communications, the value of the atmospheric attenuation coefficient changes with different weather types. The atmospheric attenuation is decided by the atmospheric particle size. In good weather, the atmospheric particle size is relatively small. In bad weather, however, the atmospheric particle size is relatively large. In a free-space transmission of 200 m, the atmospheric attenuation varies from 0.5 dB (good weather) to 50 dB (bad weather) [31]. In this demonstration, an atmospheric attenuation of 0.5 dB occurs, which is far less than the worst case of 50 dB/200 m.

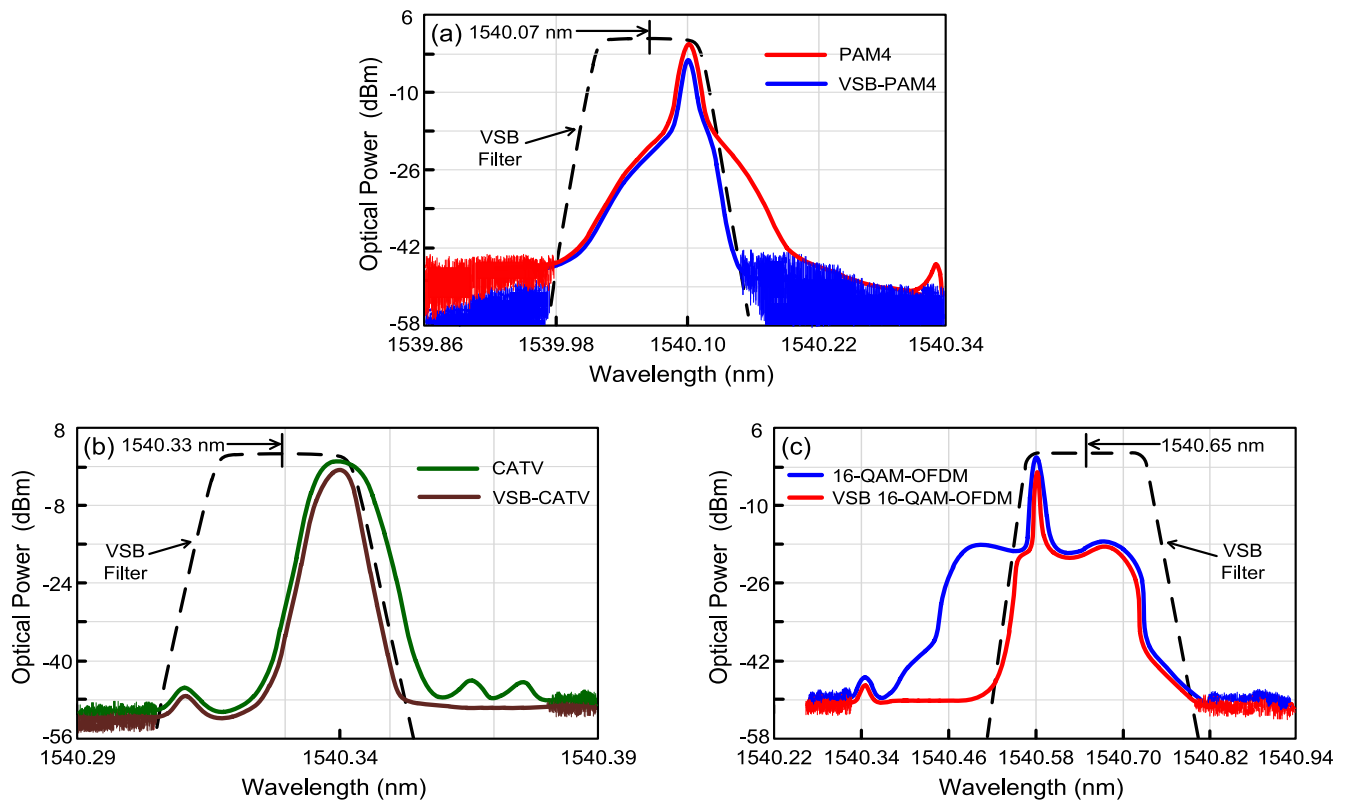
### III. RESULTS AND DISCUSSIONS

Fig. 3 displays the optical spectra of three wavelengths with 60 Gb/s PAM4 ( $y$ -polarization), 50–550 MHz CATV even-channel (polarization rotated at a  $45^\circ$  angle to the  $x$ -axis), and 70 Gb/s 16-QAM-OFDM ( $x$ -polarization) signals.

These three wavelengths have different polarizations and are spaced by 30 GHz. Regarding interference caused by polarization crosstalk, it can be eliminated by adopting a triple-polarization scheme. For three wavelengths with different polarizations, interference induced by polarization crosstalk will not worsen system's performance because the polarization crosstalk will be negligibly small. Moreover, the optical spectra of 60 Gb/s PAM4 and VSB-PAM4 ( $y$ -polarization), 50–550 MHz CATV and VSB-CATV (polarization rotated at a  $45^\circ$  angle to the  $x$ -axis), and 70 Gb/s 16-QAM-OFDM and VSB 16-QAM-OFDM ( $x$ -polarization) signals are presented in Figs. 4(a), 4(b), and 4(c), respectively. With the utilization of polarization-independent TOBPF, three polarized wavelengths modulated at different wavelengths are de-multiplexed. Polarization-tracking free de-multiplexing is achieved when other polarized wavelengths are filtered out. It is worth mentioning that TOBPF removes the requirement for complicated polarization de-multiplexing mechanism. In addition, the TOBPF works as an optical VSB filter as well. Optical VSB filter, which can remove optical signal's additional linewidth, is deployed to eliminate the fiber dispersion resulted from the 40 km SMF transport. As the optical VSB filter's central wavelength is located at 1540.07/1540.33/1540.65 nm, the optical PAM4/CATV/16-QAM-OFDM signal's spectrum on the right/right/left side is partly lessened to generate optical VSB-PAM4/VSB-CATV/VSB 16-QAM-OFDM signal.



**FIGURE 3.** The optical spectra of three wavelengths with 60 Gb/s PAM4 (y-polarization), 50–550 MHz CATV even-channel (polarization rotated at a 45° angle to the x-axis), and 70 Gb/s 16-QAM-OFDM (x-polarization) signals.



**FIGURE 4.** The optical spectra of (a) 60 Gb/s PAM4 and VSB-PAM4 (y-polarization), (b) 50–550 MHz CATV and VSB-CATV (polarization rotated at an angle of 45° to the x-axis), and (c) 70 Gb/s 16-QAM-OFDM and VSB 16-QAM-OFDM (x-polarization) signals.

The optical PAM4/CATV/16-QAM-OFDM signal owns a wide linewidth, whereas the optical VSB-PAM4/VSB-CATV/VSB 16-QAM-OFDM signal owns a narrow one. Over a span of 40 km SMF, distortions generated by fiber dispersion deteriorate the performance of hybrid fiber-FSO integrated systems owing to optical PAM4/CATV/16-QAM-OFDM signal’s widened linewidth. With the deployment of optical VSB filter, the widened optical spectra through the interaction of fiber dispersion will be partially compressed.

Accordingly, fiber dispersion induced by 40 km SMF transport can be alleviated through optical VSB-PAM4/VSB-CATV/VSB 16-QAM-OFDM modulation.

Fig. 5 presents the BER performances of 60 Gb/s PAM4 signal in the back-to-back (BTB) condition (VSB-PAM4), through a 40 km SMF transmission (VSB-PAM4), through a 40 km SMF transmission with 200 m free-space link (PAM4 and VSB-PAM4), through a 40 km SMF transmission with 250 m free-space link

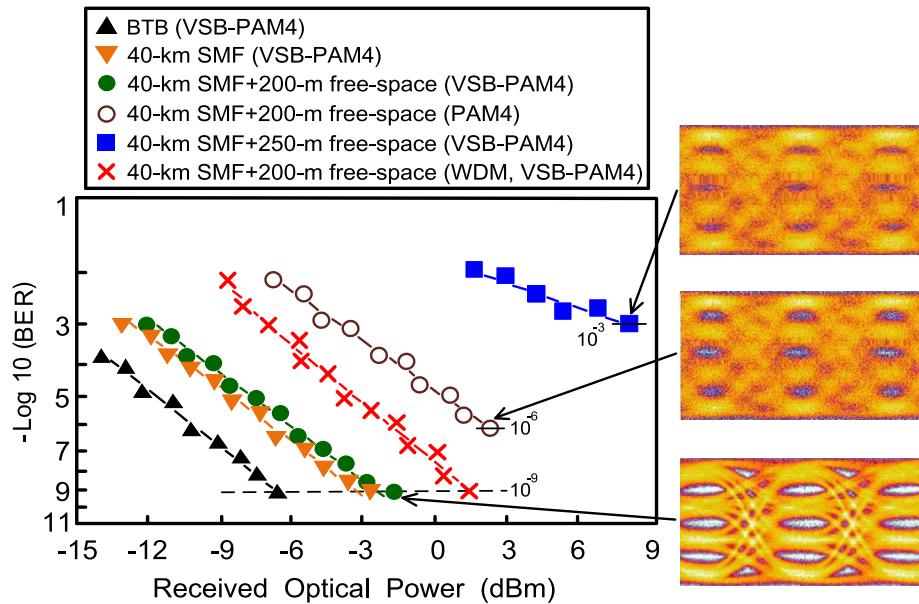


**FIGURE 5.** The BER performances of 60 Gb/s PAM4 signal in the BTB condition, through a 40 km SMF transmission (VSB-PAM4), through a 40 km SMF transmission with 200 m free-space link (PAM4 and VSB-PAM4), through a 40 km SMF transmission with 250 m free-space link (VSB-PAM4), and through a 40 km SMF transmission with 200 m free-space link (WDM, VSB-PAM4).

(VSB-PAM4), and through a 40 km SMF transmission with 200 m free-space link (wavelength-division-multiplexing (WDM), VSB-PAM4). With  $10^{-9}$  BER operation, a 4-dB power penalty occurs between the BTB condition and that through a 40 km SMF transmission (VSB-PAM4). This 4 dB power penalty arises from the adoption of an optical VSB filter to mitigate the fiber dispersion by decreasing the optical PAM4 signal's linewidth. In addition, with  $10^{-9}$  BER operation, a 1.1-dB power penalty exists between the condition through a 40 km SMF transmission (VSB-PAM4) and that through a 40 km SMF transmission with 200 m free-space link (VSB-PAM4). This 1.1-dB power penalty can be ascribed to the atmospheric attenuation because of 200 m free-space transmission, and coupling loss for coupling laser light from doublet lens 2 to fiber's ferrule. And further, with optical PAM4 modulation, the BER is greatly demoted to  $10^{-6}$  (from  $10^{-9}$  to  $10^{-6}$ ). This poor BER performance is owing to the fiber dispersion associated with 40 km SMF transmission, atmospheric attenuation because of the 200 m free-space link, and coupling loss from the laser beam being coupled from doublet lens 2 to fiber's ferrule [32], [33]. Over a 40-km SMF span, distortions produced by fiber dispersion deteriorate the BER performance by reason of the innate trait of the optical PAM4 signal with wide linewidth. As for the three wavelengths with single polarization (WDM, VSB-PAM4), the power penalty increases by about 3.2 dB, compared with the condition of three wavelengths with different polarizations (VSB-PAM4). This 3.2 dB power penalty increment is attributable to the distortions induced by the beating among the three parallel polarized wavelengths. For three wavelengths with single polarization and a close channel spacing of 30 GHz, distortions produced

by the beating among the three wavelengths degrade system's performance. If a 40-GHz channel spacing exists in a WDM scenario (a 40-GHz RF signal is supplied to the first MZM), distortions produced by the beating will be further reduced and system's performance will be further improved. However, a costly 40-GHz RF signal generator is required and a broad spectral width (reduced spectral efficiency) is obtained. In comparison with WDM scenario, polarization multiplexing scenario is worth using because it can automatically reject distortions produced by the three parallel wavelengths. Furthermore, as the free-space transmission increases to 250 m (VSB-PAM4), the BER declines to  $10^{-3}$  because of larger coupling loss at the receiving side, as compared to that of the 200 m free-space link. The laser beam emitted from doublet lens 1 will be expanded as it communicates through 250 m free-space link. With an expanded laser beam, light passes through the doublet lens 2 will be reduced. The optical power received by the PD is noticeably decreased, resulting in poor BER performance. The eye diagrams of 60 Gb/s PAM4/VSB-PAM4 signal through a 40 km SMF transmission with 200 m/250 m free-space link are displayed in Fig. 5 as well. Through a 40 km SMF transmission with 200 m free-space link (VSB-PAM4), clear eye diagrams are obtained. In the state of through a 40 km SMF transmission with 200 m free-space link (PAM4), amplitude and phase fluctuations are observed in the eye diagrams. Through a 40 km SMF transmission with 250 m free-space link (VSB-PAM4), however, close eye diagrams obviously exist.

The CSO and CTB values of BTB (VSB-CATV), through 40 km SMF transport (VSB-CATV), through 40 km SMF transport and 200 m free-space transmission (CATV and

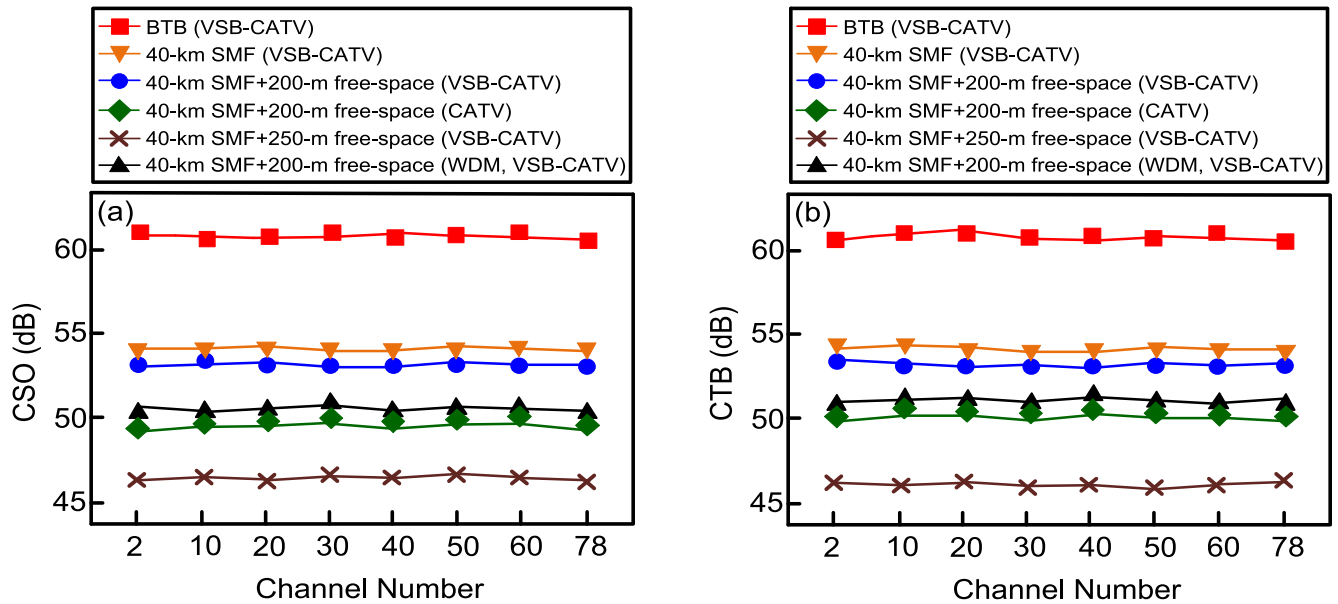


**FIGURE 6.** The (a) CSO and (b) CTB values of BTB (VSB-CATV), through 40 km SMF transport (VSB-CATV), through 40 km SMF transport and 200 m free-space transmission (CATV and VSB-CATV), through 40 km SMF transport and 250 m free-space transmission (VSB-CATV), and through 40 km SMF transport and 200 m free-space transmission (WDM, VSB-CATV).

VSB-CATV), through 40 km SMF transport and 250 m free-space transmission (VSB-CATV), and through 40 km SMF transport and 200 m free-space transmission (WDM, VSB-CATV) are shown in Figs. 6(a) and 6(b), respectively. For the scenario through 40 km SMF transport and 200 m free-space transmission (VSB-CATV), the CSO/CTB values are degraded about 1.1/1 dB, compared with that through 40 km SMF transport (VSB-CATV). These CSO/CTB degradations are attributed to the atmospheric attenuation due to 200 m free-space transmission and coupling loss between doublet lens 2 and fiber's ferrule. As the free-space transmission distance is 200 m, with optical CATV modulation, it is to be observed that the CSO/CTB values ( $\geq 49.6/50$  dB) do not satisfy the end-user CSO/CTB requirements ( $\geq 53/53$  dB) [30]. With optical VSB-CATV modulation, nevertheless, the CSO/CTB values ( $\geq 53/53.4$  dB) do meet the end-user demands. These improved results are ascribed to the adoption of optical VSB filter to reduce the optical CATV signal's linewidth. As the free-space transmission distance increases to 250 m (VSB-CATV), considerable CSO/CTB degradations of 6.8/7 dB exist between the states of through a 40 km SMF transport with 200 m and 250 m free-space transmissions. These considerable CSO/CTB degradations are primarily attributable to higher coupling loss at the receiving end. Additionally, for the three wavelengths with single polarization (WDM, VSB-CATV), it is to be found that the CSO/CTB values with single polarization are reduced by about 2.9/2.9 dB, respectively, in comparison with systems with different polarizations (VSB-CATV). These CSO/CTB reductions result from the distortions induced by the beating among the three parallel polarized wavelengths. Adopting three wavelengths with different polarizations can

dramatically avoid distortions produced by the three parallel polarized wavelengths, resulting in better CSO and CTB performances.

Figs. 7(a)-7(f) display the BER values and constellation maps of the 70 Gb/s 16-QAM-OFDM signal in the BTB state (VSB 16-QAM-OFDM/7(a)), through a 40-km SMF span (VSB 16-QAM-OFDM/7(b)), through a 40-km SMF span with 200-m free-space transmission (VSB 16-QAM-OFDM/7(c) and 16-QAM-OFDM/7(d)), through a 40-km SMF span with 250-m free-space transmission (VSB 16-QAM-OFDM/7(e)), and through a 40-km SMF span with 200-m free-space transmission (WDM, VSB 16-QAM-OFDM/7(f)), respectively. In the BTB state [Fig. 7(a)], a low BER of  $8.2 \times 10^{-6}$  and a clear constellation map are achieved. Through a 40-km SMF span, a BER of  $7.8 \times 10^{-5}$  and a still clear constellation map are achieved with optical VSB 16-QAM-OFDM modulation [Fig. 7(b)]. Through a 40-km SMF span with 200-m free-space transmission, a BER of  $4.6 \times 10^{-4}$  and a somewhat clear constellation map are acquired with optical VSB 16-QAM-OFDM modulation [Fig. 7(c)]. The achieved BER is under the forward error correction limit standard of  $3.8 \times 10^{-3}$ . Low BER and somewhat clear constellation map demonstrate the practicality of delivering a 70 Gbps 16-QAM-OFDM data signal in fiber-FSO integrated systems. Through a 40-km SMF span with 200-m free-space transmission, however, a higher BER of  $8.6 \times 10^{-3}$  and a somewhat turbid constellation map are attained with optical 16-QAM-OFDM modulation [Fig. 7(d)]. These declines in BER performance and constellation map quality chiefly result from the disuse of an optical VSB filter so as not to lower fiber dispersion-induced distortions. Furthermore, as



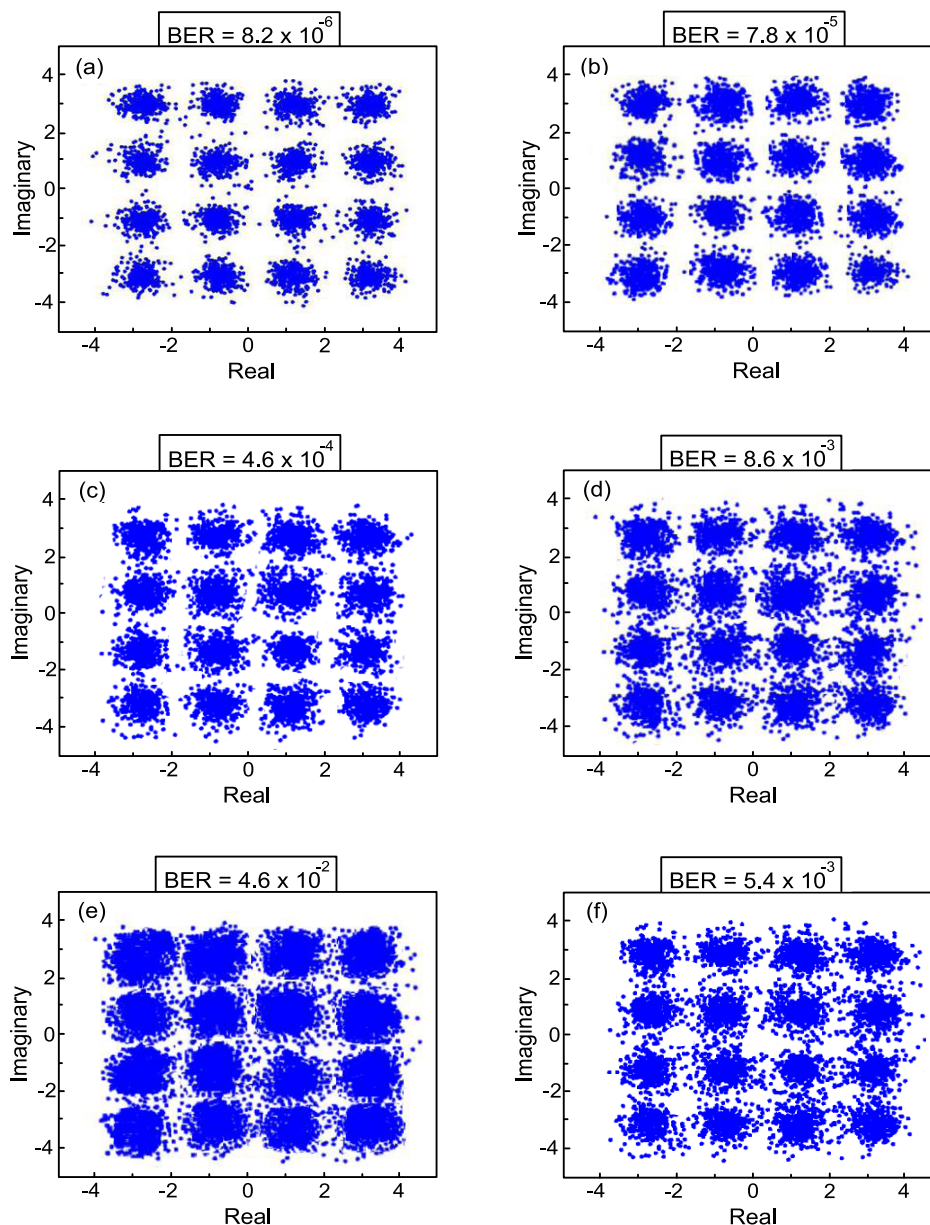


**FIGURE 7.** The BER values and constellation maps of 70 Gb/s 16-QAM-OFDM signal (a) in the BTB state (VSB 16-QAM-OFDM), (b) through a 40-km SMF span (VSB 16-QAM-OFDM), (c) through a 40-km SMF span with 200-m free-space transmission (VSB 16-QAM-OFDM), (d) through a 40-km SMF span with 200-m free-space transmission (16-QAM-OFDM), (e) through a 40-km SMF span with 250-m free-space transmission (VSB 16-QAM-OFDM), and (f) through a 40-km SMF span with 200-m free-space transmission (WDM, VSB 16-QAM-OFDM).

the free-space optical link increases to 250 m [Fig. 7(e)], a high BER of  $4.6 \times 10^{-2}$  and a turbid constellation map exist due to the considerable coupling loss on doublet lens 2 and the receiver receiving less light. Moreover, for three parallel wavelengths (WDM, VSB 16-QAM-OFDM) [Fig. 7(f)], a BER of  $5.4 \times 10^{-3}$  and a slightly turbid constellation map are obtained. Compared with systems with three different polarized wavelengths (VSB 16-QAM-OFDM), the BER performance is degraded ( $4.6 \times 10^{-4} \rightarrow 5.4 \times 10^{-3}$ ) and the constellation map becomes less clear. These degradations mainly

arise from the distortions due to the beating among the three parallel wavelengths.

#### IV. SUMMARY AND CONCLUSION

A hybrid Internet/CATV/5G fiber-FSO integrated system with a triple-wavelength polarization multiplexing scenario was successfully demonstrated for the first time. In the triple-wavelength polarization multiplexing scenario with VSB PAM4/CATV/16-QAM-OFDM modulation, the channel capacity and transmission performance can be

considerably enhanced. By utilizing a TOBPF, the polarized wavelengths are simply de-multiplexed from the polarization multiplexing scenario, and the optical VSB PAM4/CATV/16-QAM-OFDM signal is feasibly produced to decrease the fiber dispersion-induced distortions. In comparison with traditional polarization multiplexing fiber-FSO integrated systems with sophisticated polarization de-multiplexing mechanism, our proposed system exhibits the advantages of low complexity as well as flexibility. Competent BER performance, qualified PAM4 eye diagrams, clear constellation map, and good CSO/CTB performance are achieved through a 40 km SMF transmission with 200 m free-space link. This illustrated hybrid fiber-FSO integrated system is a promising integration into which not only optical fiber backhaul and optical wireless feeder networks are incorporated, but also the complex polarization-tracking mechanism is not needed and the fiber dispersion effect is mitigated. It shows the way to speed up the extensive applications through SMF transport with free-space transmission.

## REFERENCES

- [1] L. Y. Wei, C. W. Hsu, C. W. Chow, and C. H. Yeh, "40-Gbit/s visible light communication using polarization-multiplexed R/G/B laser diodes with 2-m free-space transmission," in *Proc. Conf. Opt. Fiber Commun. (OFC)*, Mar. 2019, pp. 1–3, Paper M3I.3.
- [2] C. Y. Li, H.-H. Lu, C.-W. Su, H.-W. Chen, Y.-N. Chen, Y.-R. Wu, and C.-W. Hung, "Real-time PAM4 fiber-IVLLC and fiber-wireless hybrid system with parallel/orthogonally polarized dual-wavelength scheme," *OSA Continuum*, vol. 1, no. 2, pp. 320–331, Oct. 2018.
- [3] G. Xie, F. Wang, A. Dang, and H. Guo, "A novel polarization-multiplexing system for free-space optical links," *IEEE Photon. Technol. Lett.*, vol. 23, no. 20, pp. 1484–1486, Oct. 15, 2011.
- [4] D. Fujimoto, H.-H. Lu, K. Kumamoto, S.-E. Tsai, Q.-P. Huang, and J.-Y. Xie, "Phase-modulated hybrid high-speed Internet/WiFi/Pre-5G in-building networks over SMF and PCF with GI-POF/IVLLC transport," *IEEE Access*, vol. 7, pp. 90620–90629, Jul. 2019.
- [5] W.-S. Tsai, H.-H. Lu, Y.-C. Huang, S.-C. Tu, and Q.-P. Huang, "A PDM-based bi-directional fibre-FSO integration with two RSOAs scheme," *Sci. Rep.*, vol. 9, Jun. 2019, Art. no. 8317.
- [6] C. Y. Li, H.-H. Lu, C.-W. Su, H.-W. Chen, Y.-N. Chen, Y.-R. Wu, and C.-W. Hung, "A flexible two-way PM-based fiber-FSO convergence system," *IEEE Photon. J.*, vol. 10, no. 2, Apr. 2018, Art. no. 7901509.
- [7] J. Zhang, J. Wang, Y. Xu, M. Xu, F. Lu, L. Cheng, J. Yu, and G.-K. Chang, "Fiber-wireless integrated mobile backhaul network based on a hybrid millimeter-wave and free-space-optics architecture with an adaptive diversity combining technique," *Opt. Lett.*, vol. 41, no. 9, pp. 1909–1912, May 2016.
- [8] D. Kotani, "An architecture of a network controller for QoS management in home networks with lots of IoT devices and services," in *Proc. IEEE Annu. Consum. Commun. Netw. Conf. (CCNC)*, Jan. 2019, pp. 1–4.
- [9] M. Araújo, L. Ekenberg, and J. Confraria, "Rural networks cost comparison between 5G (mobile) and FTTx (fixed) scenarios," in *Proc. IEEE Annu. Int. Symp. Pers., Indoor, Mobile Radio Commun. (PIMRC)*, Sep. 2018, pp. 259–264.
- [10] M. Carmo, S. Jardim, A. Neto, R. Aguiar, D. Corujo, and J. J. P. C. Rodrigues, "Slicing WiFi WLAN-sharing access infrastructures to enhance ultra-dense 5G networking," in *Proc. IEEE Int. Conf. Commun. (ICC)*, May 2018, pp. 1–6.
- [11] S.-H. Lee, M.-S. Yoon, S.-H. Cho, and H.-K. Cho, "Study on simplified test bench for QoS analysis using traffic models of Pre-5G service," in *Proc. IEEE Int. Conf. Ubiquitous Future Netw. (ICUFN)*, Jul. 2018, pp. 902–905.
- [12] A. E. Morra, K. Ahmed, and S. Hranilovic, "Impact of fiber nonlinearity on 5G backhauling via mixed FSO/fiber network," *IEEE Access*, vol. 5, pp. 19942–19950, 2017.
- [13] W. S. Tsai, H. H. Lu, C. W. Su, Z. H. Wang, and C. Y. Li, "Centralized-light-source two-way PAM8/PAM4 FSO communications with parallel optical injection locking operation," *IEEE Access*, vol. 7, pp. 36948–36957, 2019.
- [14] G. W. Lu, R. S. Luís, H. Toda, J. Cui, T. Sakamoto, H. Wang, Y. Ji, and N. Yamamoto, "Flexible generation of 28 Gbps PAM4 60 GHz/80 GHz radio over fiber signal by injection locking of direct multilevel modulated laser to spacing-tunable two-tone light," *Opt. Express*, vol. 26, no. 16, pp. 20603–20613, Aug. 2018.
- [15] Y. Tong, Q. Zhang, X. Wu, C. Shu, and H. K. Tsang, "112 Gb/s 16-QAM OFDM for 80-km data center interconnects using silicon Photonic integrated circuits and Kramers–Kronig detection," *IEEE/OSA J. Lightw. Technol.*, vol. 37, no. 14, pp. 3532–3538, Jul. 15, 2019.
- [16] J. Zhang, J. Yu, X. Li, Y. Wei, K. Wang, L. Zhao, W. Zhou, M. Kong, X. Pan, B. Liu, and X. Xin, "100 Gbit/s VSB-PAM-n IM/DD transmission system based on 10 GHz DML with optical filtering and joint nonlinear equalization," *Opt. Express*, vol. 27, no. 5, pp. 6098–6105, Feb. 2019.
- [17] H. Y. Chen, J. Lee, N. Kaneda, J. Chen, and Y. K. Chen, "Comparison of VSB PAM4 and OOK signal in an EML-based 80-km transmission system," *IEEE Photon. Technol. Lett.*, vol. 29, no. 23, pp. 2063–2066, Dec. 1, 2017.
- [18] S. Endo, K. I. A. Sampath, and J. Maeda, "Chromatic dispersion-based modulation distortion compensation for analog radio-over-fiber: Performance improvement in OFDM transmission," *IEEE/OSA J. Lightw. Technol.*, vol. 36, no. 24, pp. 5963–5968, Dec. 15, 2018.
- [19] H.-H. Lu, W.-J. Wang, and W.-S. Tsai, "CSO/CTB performances improvement in a bi-directional DWDM CATV system," *IEEE Trans. Broadcast.*, vol. 50, no. 4, pp. 377–381, Dec. 2004.
- [20] Y. Zhu, M. Jiang, and F. Zhang, "Direct detection of polarization multiplexed single sideband signals with orthogonal offset carriers," *Opt. Express*, vol. 26, no. 12, pp. 15887–15898, Jun. 2018.
- [21] X. Li, J. Yu, K. Wang, W. Zhou, and J. Zhang, "Photonics-aided 2×2 MIMO wireless terahertz-wave signal transmission system with optical polarization multiplexing," *Opt. Express*, vol. 25, no. 26, pp. 33236–33242, Dec. 2017.
- [22] D. Qian, N. Cvijetic, J. Hu, and T. Wang, "108 Gb/s OFDMA-PON with polarization multiplexing and direct detection," *J. Lightw. Technol.*, vol. 28, no. 4, pp. 484–493, Feb. 15, 2010.
- [23] I. B. Djordjevic, L. Xu, and T. Wang, "Beyond 100 Gb/s optical transmission based on polarization multiplexed coded-OFDM with coherent detection," *IEEE/OSA J. Opt. Commun. Netw.*, vol. 1, no. 1, pp. 50–56, Jun. 2009.
- [24] Q. Xiang, Y. Yang, Q. Zhang, and Y. Yao, "Low complexity, modulation-transparent and joint polarization and phase tracking scheme based on the nonlinear principal component analysis," *Opt. Express*, vol. 27, no. 13, pp. 17968–17978, Jun. 2019.
- [25] J. Li, T. Zeng, X. Li, L. Meng, M. Luo, Z. He, and S. Yu, "Real-time fast polarization tracking based on polarization phase locking least mean square algorithm," *Opt. Express*, vol. 27, no. 16, pp. 22116–22126, Aug. 2019.
- [26] T. Matsuda, T. Homemoto, and K. Matsumura, "Polarization multiplexing and demultiplexing technique for large capacity small optical module by using optical interleaver," in *Proc. IEEE Photon. Conf. (IPC)*, Oct. 2018, pp. 1–2.
- [27] T. Su, J. Zheng, Z. Wu, M. Zhang, X. Chen, and G.-K. Chang, "Bidirectional multiband radio-over-fiber system based on polarization multiplexing and wavelength reuse," *Opt. Express*, vol. 23, no. 8, pp. 9772–9776, 2015.
- [28] S. Shen, J.-H. Yan, P.-C. Peng, C.-W. Hsu, Q. Zhou, S. Liu, R. Zhang, K.-M. Feng, J. Finkelstein, and G.-K. Chang, "Polarization-tracking-free PDM supporting hybrid digital-analog transport for fixed-mobile systems," *IEEE Photon. Technol. Lett.*, vol. 31, no. 1, pp. 54–57, Jan. 2019.
- [29] S. J. Liu, J. H. Yan, C. Y. Tseng, and K. M. Feng, "Polarization-tracking-free PDM IF-over-fiber mobile fronthaul employing multiband DDO-OFDM," in *Proc. Conf. Lasers Electro-Opt. (CLEO)*, May 2016, pp. 1–2, Paper SF2F.3.
- [30] H. H. Lu, H.-W. Wu, C.-Y. Li, C.-M. Ho, Z.-Y. Yang, M.-T. Cheng, and C.-K. Lu, "Bidirectional fiber-IVLLC and fiber-wireless convergence system with two orthogonally polarized optical sidebands," *Opt. Express*, vol. 25, no. 9, pp. 9743–9754, May 2017.
- [31] I. I. Kim, B. McArthur, and E. J. Korevaar, "Comparison of laser beam propagation at 785 nm and 1550 nm in fog and haze for optical wireless communications," *Proc. SPIE*, vol. 4214, pp. 26–37, Feb. 2001.
- [32] C.-Y. Li, H.-H. Lu, T.-C. Lu, C.-J. Wu, C.-A. Chu, H.-H. Lin, and M.-T. Cheng, "A 100 m/320 Gbps SDM FSO link with a doublet lens scheme," *Laser Phys. Lett.*, vol. 13, no. 7, p. 075201, Jun. 2016.
- [33] X. Liu, X. Cai, S. Chang, and C. P. Grover, "Cemented doublet lens with an extended focal depth," *Opt. Express*, vol. 13, no. 2, pp. 552–557, Jan. 2005.



**CHUNG-YI LI** received the M.S. and Ph.D. degrees from the Department of Electro-Optical Engineering, National Taipei University of Technology (NTUT), Taiwan, in 2008 and 2012, respectively. From 2013 to 2014, he was an Engineer with the Innovation and Product Development Department, FOCI Fiber Optic Communications, Inc., Hsinchu, Taiwan. He has been with the Department of Electro-Optical Engineering, NTUT, as a Research Assistant Professor, since 2014. He has also been with the Department of Communication Engineering, National Taipei University (NTU), as an Assistant Professor, since 2018. His research interests include FSO communications, UWOC, and fiber-FSO convergence.



**HSIAO-WEN WU** received the M.S. and Ph.D. degrees from the Department of Electrical and Computer Engineering, Marquette University, USA, in 2000. Since 2000, she has been with the Department of Electronics Engineering, Tunghnan University, Taipei, Taiwan, as an Assistant Professor. Her research interests include FSO communications, fiber-FSO convergence, and speech quality in telecommunications.



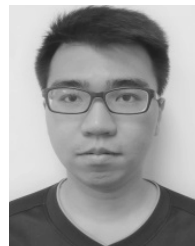
**HAI-HAN LU** (SM'08) received the M.S. and Ph.D. degrees from the Institute of Electro-Optical Engineering, National Central University, Taiwan, in 1991 and 2000, respectively.

He has been with the Department of Electro-Optical Engineering, National Taipei University of Technology (NTUT), as an Associate Professor, since 2003. He has promoted to Professor, Distinguished Professor, and Lifetime Distinguished Professor in 2003, 2006, and 2017, respectively.

He has authored or coauthored more than 200 articles in SCI cited international journals and more than 130 articles in international conferences. His research interests include FSO communications, UWOC transport systems, FSO-UWOC convergence, fiber-FSO convergence, and PAM4/PAM8 transmission systems. He is currently a Fellow of SPIE, a Fellow of IET, and a Senior Member of OSA. He received the Sun Yat-sen Academic Award (Natural Science, 2017), the National Invention Award (Gold Medal, 2016), the ICT Month Innovative Elite Products Award, in 2014 and 2016, the Outstanding Electrical Engineering Professor Award of the Chinese Institute of Engineering, in 2015, the Outstanding Engineering Professor Award of the Chinese Engineer Association, in 2013, and the Outstanding Research Award of NTUT, in 2004, for his significant technical contributions to FSO communications, PAM4/PAM8 transmission systems, fiber-FSO convergence, and fiber-wireless convergence.



**WEN-SHING TSAI** received the M.S. and Ph.D. degrees from the Department of Electro-Optical Engineering, National Taipei University of Technology (NTUT), Taiwan, in 2003 and 2006, respectively. He has been with the Department of Electrical Engineering, Ming Chi University of Technology, as an Assistant Professor, since 2006. He has promoted to Associate Professor, in 2012. His research interests include FSO communications, fiber-FSO convergent systems, and PAM8/PAM4 transmission systems.



**SONG-EN TSAI** was born in New Taipei City, Taiwan, in December 1995. He received the B.S. degree from the National Yunlin University of Science and Technology (YunTech), Yunlin, Taiwan, in 2018. He is currently pursuing the M.S. degree with the Institute of Electro-Optical Engineering, National Taipei University of Technology (NTUT), Taiwan. His research interests include PAM4 transmission systems, FSO communications, and fiber-FSO convergence.



**JING-YAN XIE** was born in Changhua, Taiwan, in September 1995. He received the B.S. degree from the National Yunlin University of Science and Technology, Yunlin, Taiwan, in 2018. He is currently pursuing the M.S. degree with the Institute of Electro-Optical Engineering, National Taipei University of Technology (NTUT), Taiwan. His research interests include PAM4 transmission systems and fiber-FSO and fiber-wireless convergences.

...